Available online at www.sciencedirect.com
SCIENCE DIRECT
Biochemical and Biophysical Research Communications 339 (2006) 172–179
BBRC
www.elsevier.com/locate/ybbrc

Microtubule-associated protein 8 contains two microtubule binding sites

Jianqing Ding, Angela Valle, Elizabeth Allen, Wei Wang, Timothy Nardine, Yingjiu Zhang, Lily Peng, Yanmin Yang *

Department of Neurology and Neurological Sciences, Stanford University School of Medicine, 1201 Welch Road, Stanford, CA 94305-5489, USA

Received 20 October 2005
Available online 10 November 2005

Abstract

Microtubule-associated proteins (MAPs) are critical regulators of microtubule dynamics and functions, and have long been proposed to be essential for many cellular events including neuronal morphogenesis and functional maintenance. In this study, we report the characterization of a new microtubule-associated protein, we named MAP8. The protein of MAP8 is mainly restricted to the nervous system postnatally in mouse. Its expression could first be detected as early as at embryonic day 10, levels plateau during late embryonic and neonatal periods, and subsequently decrease moderately to remain constant into adulthood. In addition to its carboxyl terminal binding site, the MAP8 polyprotein also contains a functional microtubule-binding domain at its N-terminal segment. The association of the carboxyl terminal of the light chain with actin microfilaments could also be detected. Our findings define MAP8 as a novel microtubule associated protein containing two microtubule binding domains.

Keywords: Microtubules; Microtubule-associated protein; Cytoskeleted organization; Actin filament

During the development and throughout life, microtubules are essential cytoskeletal components in eukaryotic cells where they play vital roles in various cellular events, from controlling protein translation to trafficking, cellular signaling to morphogenesis, and differentiation. Microtubules are especially abundant in neurons where they are linked together by a diverse family of associated proteins whose interactions with microtubules or other cytoskeletal proteins are functionally regulated [1,2]. Over the past several decades, a number of microtubule associated proteins (MAP), such as the MAP5/MAP1B, MAP2, and tau families, have been discovered and intensively characterized. MAP5/MAP1B, which shares many common structural features with MAP1A, is the first MAP expressed during development of the nervous system, and postnatally its expression in some tissues is down-regulated dramatically, while that of MAP1A increases[3]. In addition to microtubule binding, MAP5/MAP1B also interacts with actin microfilaments, gigaxonin, and myelin associated glycoprotein[4–8]. MAP2 has three isoforms, MAP2A, B, and C, and is mainly present in cell body and dendrites of neurons (for review, see[9]). Tau is another classic MAP that stabilizes microtubules and is enriched in axons [10].

MAPs are considered to be essential for microtubule functions in many cellular processes in the nervous system. MAP5/MAP1B deficient mice have shown abnormal developmental defects in brain architecture including delayed myelination, reduced axon caliber, tract malformation, and layer disorganization [11–14]. However, the loss of a single MAP protein appears to be compensated by the functional redundancy among classical MAPs, since the phenotype of double MAP knockout mice is markedly more severe [15]. In contrast, however, abundant evidence demonstrates that the overexpression/accumulation of MAPs contributes significantly to the pathogenesis of neurodegeneration and cell death. While MAP2 null mice fail to display abnormal cytoarchitecture of their nervous system [15], MAP2 overexpression was implicated in neuronal migration disorders [16]. Tau null mice were indistinguishable from control littermates for axonal extension[17],

* Correspondence author. Fax: +1 650 498 6262.
E-mail address: yanmin.yang@stanford.edu (Y. Yang).

0006-291X/$ - see front matter © 2005 Elsevier Inc. All rights reserved.
doi:10.1016/j.bbrc.2005.10.199

whereas Tau overexpression results in a severe neuropathy in transgenic mice [18,19]. Moreover, its role in the pathogenesis of neurodegenerative disorders, such as Parkinson's and Alzheimer's, has long been demonstrated [20–22]. In addition, delayed postnatal downregulation of MAP5/MAP1B has been linked to mental retardation in fragile X syndrome [23,24].

In this study, we report the characterization of a neuronal specific microtubule associated protein we have named MAP8. The deduced amino acid sequence reveals an average 27% homology with classical MAP5/MAP1B or 1A. At all developmental stages, MAP8 could be detected in the nervous system as early as mouse embryonic day 10. Protein level is most abundant in fetal and neonatal stages, and postnatally MAP8 expression subsequently decreases, but remains constant into adulthood. The polypeptide precursor of MAP8 is cleaved in vivo into a ~120 kDa heavy chain and a ~30 kDa light chain, each containing a functional microtubule-binding domain. The carboxyl terminal of MAP8 light chain additionally binds actin microfilaments. The immunohistochemical studies showed that MAP8 is present in both cell bodies and their processes during the development. The characterization of MAP8 protein improves our understanding of cytoskeletal constituents and their physiological functions.

Materials and methods

Generation of antibodies. A purified GST fusion protein encompassing N-terminal portion of the light chain or a synthetic peptide located within the heavy chain was used for raising anti-M8-C or anti-M8-N antibodies in rabbits, respectively. The antisera were affinity purified and tested against purified recombinant protein or total cell lysates from Flag-M8-HC or Flag-M8-LC transfected cells prior to use.

Immunohistochemistry. Immunohistochemistry with MAP8 antibody was performed using Vector ABC-AP kit (Vector Laboratories, Burlingame). Newborn mice were sacrificed by using CO_2 and fixed for 8 h to overnight in 4% paraformaldehyde in 0.1 M PB (pH 7.4)at 4 °C, followed by decalcification. Brain and other nervous tissue were removed and processed for paraffin embedding. The tissue blocks were cut in 10–20 μm sections, fixed for 30 min, and blocked for 1 h. Anti-M8-N or anti-M8-C were diluted at 1:100 or 1:50, respectively, and added to the slides for 2 h at room temperature. After washing, the sections were then incubated in biotinylated goat anti-rabbit for 1 h (1:200, Vector laboratories), washed again, and then placed in the ABC-AP reagent for 1 h. Samples were detected using the NBT/BCIP solution according to manufacturer's instructions.

Protein purification and microtubule binding assays. Overnight bacterial cultures of GST-MTBD-N or GST-MTBD-C were collected and the total cell lysates were prepared. GSH-conjugated Sepharose beads were used for purifying soluble recombinant proteins, and the purified fusion proteins were analyzed on 10% SDS–polyacrylamide gel electrophoresis (SDS–PAGE). The concentrations of the two fusion proteins were determined using the Bradford protein assay.

Microtubule binding studies were carried out using purified recombinant fusion proteins and microtubules (Cytoskeleton). The assays were performed by measuring co-sedimentation of taxol-stabilized microtubules (50 μM) and GST-MTBD-N (5.2 μM) or GST-MTBD-C (6.0 μM) by ultracentrifugation (Beckman TL 100) of 50-μl samples. Aliquots of the supernatant and pellet fractions were separated by electrophoresis through 10% SDS–PAGE, which were then stained with Coomassie blue to visualize protein. Scanning densitometry of dried gels was used for quantification of protein. BSA or GST was analyzed in parallel as negative controls, and each assay was performed with or without polymerized microtubules.

The k_d assays for GST-MTBD-N or GST-MTBD-C were conducted as described above with GST-MTBD-N or GST-MTBD-C fusion proteins at the concentration range of 0.65–10.25 μM. Proteins were quantitated by densitometric scanning. Scatchard analyses were performed in triplicate, and results were averaged.

Results

MAP8 is expressed throughout the development and mainly in nervous tissue

Microtubule associated protein 8 (MAP8) was identified from a brain cDNA library. The deduced amino acid sequence of MAP8 is ~68% conserved between human and rodents, and shares moderate homology with the classical microtubule-associated protein 5/1B (MAP5/MAP1B) and 1A (MAP1A) at approximately 29%. The polypeptide precursor of MAP8 also contains a proline-rich proteolytic cleavage site at its carboxyl terminal (Fig. 1B, indicated by arrowhead), similar to those present in MAP5/MAP1B or MAP1A [26]. Two antibodies were raised, anti-M8-N and anti-M8-C which recognize the N-terminal and C-terminal portions of MAP8, respectively (see diagram in Fig. 1B). To analyze its protein expression pattern, and to assess whether MAP8 is processed into heavy and light chains in vivo, we constructed N-terminal FLAG-tagged expression vectors encoding full-length, heavy or light chains of MAP8 (Flag-M8-F, Flag-M8-HC, and Flag-M8-LC in Fig. 1B). All three expression vectors were transiently expressed in COS7 cells, which express little or no endogenous MAP8 (Fig. 1A, lanes 2, 5, 7, and 10), thus permitting the investigation of MAP8's cleavage without the interference of endogenous protein. As predicted, MAP8 appears to be cleaved in vivo into N-terminal heavy chain (HC) and C-terminal light chain (LC). As indicated by immunoblot analysis, the anti-M8-N antibody detects the amino terminal HC of MAP8 in mouse brain tissue with a single band at ~120 kDa (Fig. 1A, lane 3), which is smaller in size than the full-length protein of 150–160 kDa found in Flag-M8-F transfected COS7 cells (Fig. 1A, lane 1) but identical to the size of flag-M8-HC from the transfected cells (Fig. 1A, lane 4). It appears likely that COS7 cells do not express the processing enzyme that cleaves the protein. Likewise, the anti-M8-C antibody recognizes the full-length protein of Flag-M8-F from transfected cells (Fig. 1A, lane 6) and the carboxyl terminal LC of MAP8 at ~30 kDa in brain similar to the one from flag-M8-LC transfected cells (Fig. 1A, lanes 8 and 9, respectively). Notably, a ~120 kDa band was not detectable on the blot probed with anti-M8-C (Fig. 1A, lane 8), further confirming efficient proteolytic processing of MAP8 in brain. The blots were also stripped and re-probed using anti-flag antibody, and overlapping bands in the lanes of flag-tagged

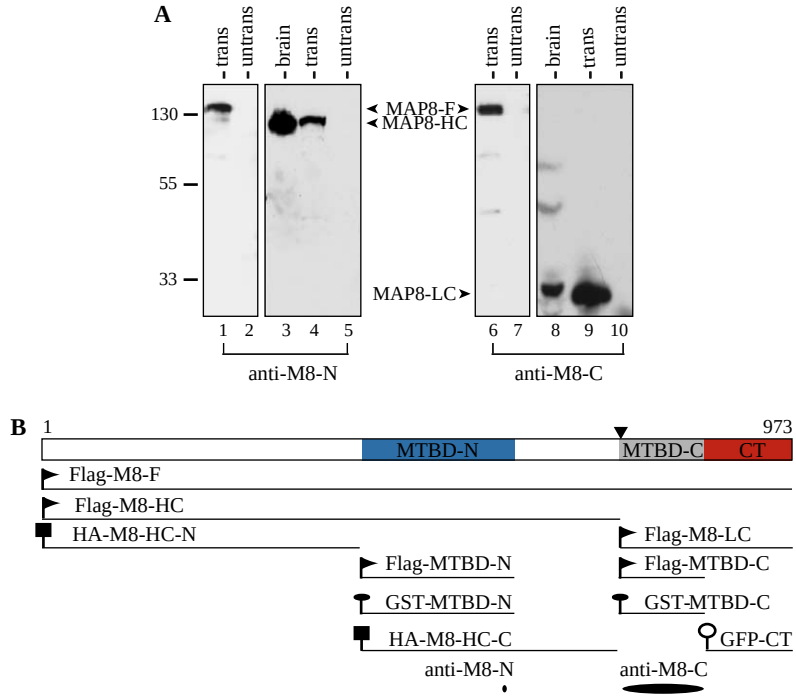

Fig. 1. Expression of MAP8. Immunoblot analysis with rabbit anti-MAP8 antibodies: anti-M8-N (A, lanes 1–5) or anti-M8-C (A, lanes 6–10). (A) The Flag-M8-F could be detected in transfected COS 7 cells with both antibodies (A, lanes 1 and 6); A ~120 kDa band was found in mouse brain tissue (lane 3) and Flag-M8-HC transfected cells (lane 4) with anti-M8-N, while a ~30 kDa band was detected by anti-M8-C (lanes 8 and 9); the untransfected COS7 cells express no endogenous MAP8 (lanes 2, 5, 7, and 10). MAP8-F, uncleaved full-length MAP8; MAP8-HC, MAP8 heavy chain; MAP8-LC, MAP8 light chain. (B) Schematic representation of the domain structures of MAP8. Individual domains, regions, and expression constructs used in this study are all illustrated. MTBD, microtubule binding domain; CT, C-terminus of the light chain. The arrowhead points to the cleavage site of the HC and LC.

full-length, HC or LC transfected cells confirmed antibody specificities (not shown). The result achieved on HC and LC expression is consistent with that of MAP1S [25].

Next we investigated the temporal and spatial MAP8 expression in mouse tissues by means of immunoblot assays. The extracts from mouse brain, spinal cord, lung, liver, heart, and muscle were probed using anti-M8-N (Fig. 2A) and anti-M8-C (not shown). In all tissues analyzed in the assay, MAP8 was mainly expressed in nervous tissues of brain and spinal cord (Fig. 2A, lanes 1 and 2). No marked or stable expression was consistently noted in other examined tissues (Fig. 2A, lanes 3–6), results different from ubiquitous expression pattern of MAP1S [25]. At all developmental stages, MAP8 could be detected as early as embryonic day 10 (Fig. 2B, lane 1). The detection of a ~150 kDa size band probably corresponds to an incomplete cleavage product of full-length MAP8 in brain at the early stage of development. The protein level subsequently increased during the late stages of embryonic development and is most abundant in fetal and neonatal stages (Fig. 2B, lanes 2–4). Postnatally, the expression of MAP8 seems moderately decreased, but remains persistent in 3-month adult brain (Fig. 2B, lane 5).

To determine the distributions of MAP8 protein in nervous system and its cellular localization within neurons, immunohistochemical analysis was conducted on neonatal mouse sections of nervous tissues. As judged by antibody labeling (anti-M8-N), MAP8 protein appears in all of the neuronal tissues examined (Figs. 2C–H). In spinal cord, the positive immunoreactivity could be found uniformly in both ventral and dorsal horns (Fig. 2C). Likewise, the neurons in hippocampus and cerebral cortex display strong MAP8 immunoreactivity (Figs. 3E and F). In cerebellum, all three layers of cortex (molecular, Purkinje, and granular cell layers) are positively stained (Figs. 2G and H). MAP8 expression can also be easily detected in the peripheral nervous system, as demonstrated by unequivocal staining of dorsal root ganglia (DRG) (Fig. 2D). Although cell bodies and processes (Fig. 2, arrows in C and H) are MAP8 positive, the protein seems to be more concentrated in the cell bodies. These studies demonstrate that expression of MAP8 in the nervous system is ubiquitous.

MAP8 contains two microtubule binding domains

Since MAP8 is homologous to classical microtubule binding proteins, we assessed whether MAP8 possesses microtubule-binding activity using transient expression of Flag-MAP8-F in COS7 cells. After confirming the Flag-MAP8-F expression with immunoblot analysis, double immunofluorescence microscopy was conducted using anti-tubulin and anti-flag. A striking microtubule decoration was observed in approximately 70% of the flag-M8-F transfected cells (Figs. 3A and B). To dissect the domain(s) responsible for microtubule association,

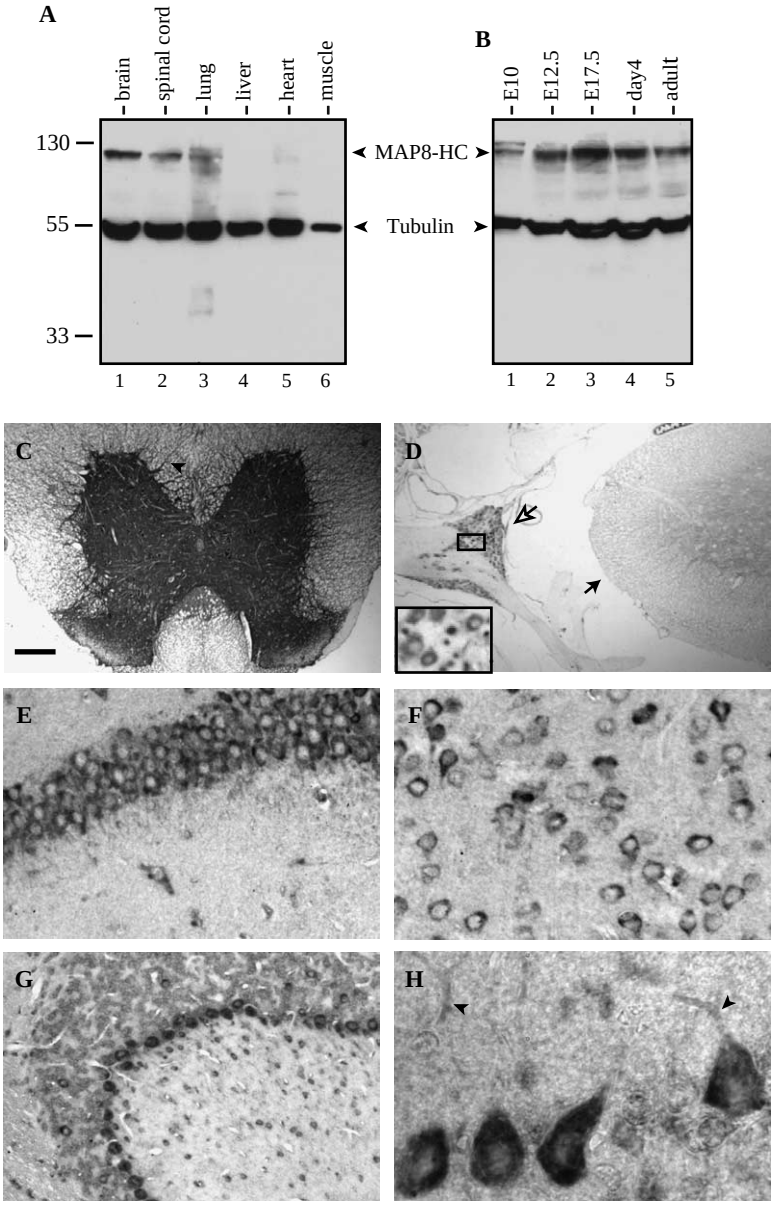

Fig. 2. Temporal and spatial expression of MAP8. (A) Immunoblot analysis with rabbit anti-M8-N on mouse tissues of postnatal 2 weeks. MAP8 protein was mainly found in the brain and spinal cord (lanes 1 and 2). It is barely detectable in other examined tissues (lanes 3–6). (B) Immunoblot analysis with rabbit anti-M8-N on mouse tissues ranging from embryo days 10 (E10) to postnatal 3 months (adult). The expression of MAP8 could be found as early as E10 (lane 1), peaked at E17.5 (lane 3), and moderately decreased in adult sample at the age of postnatal 3 months (lane 5). The higher molecular band in E10 (lane 1) probably represents the uncleaved MAP8. (C–H) Paraffin sections of mouse tissues were immunostained with anti-M8-N. Positive immunoreactivity could be found in spinal cord (C,D), dorsal root ganglia (DRG), (D and inset), hippocampus (E), cerebral cortex (F), and cerebellum (G,H). The arrowheads in (C) and (H) indicate the positively stained processes. The solid arrow in (D) points to the spinal cord and the open arrow to DRG. Bar in (C) represents 60 μm; 90 μm in (D); 12 μm in (E,F), 25 μm in (G); and 6 μm in (H).

constructs containing various portions of MAP8 as depicted in the diagram (Fig. 1B) were examined in cells for their distribution patterns. In addition to the C-terminal microtubule binding domain which was reported for MAP1S [25], the N-terminal HC also contains a binding site. As shown by double immunofluorescence microscopy, two constructs encompassing MTBD-N within the heavy chain (Flag-MTBD-N) and MTBD-C at the N-terminus of light chain (Flag-MTBD-C) co-aligned with microtubule network in transfected cells (Figs. 3C and D, and E and F, respectively). In contrast, no co-localizations between the N-terminus of HC and cytoskeletal network were observed in those transfected cells (Fig. 5C). While displaying no microtubule association, the C-terminus of MAP8 light chain, GFP-CT, reveals an actin binding capacity. In approximately 67% of the transfected cells, GFP-CT protein displayed intracellular aggregates or a diffuse distribution pattern. However, in approximately 33% of the GFP-CT expressing cells the protein co-aligned with actin stress fibers (Figs. 3G and H), similar to the C-terminus

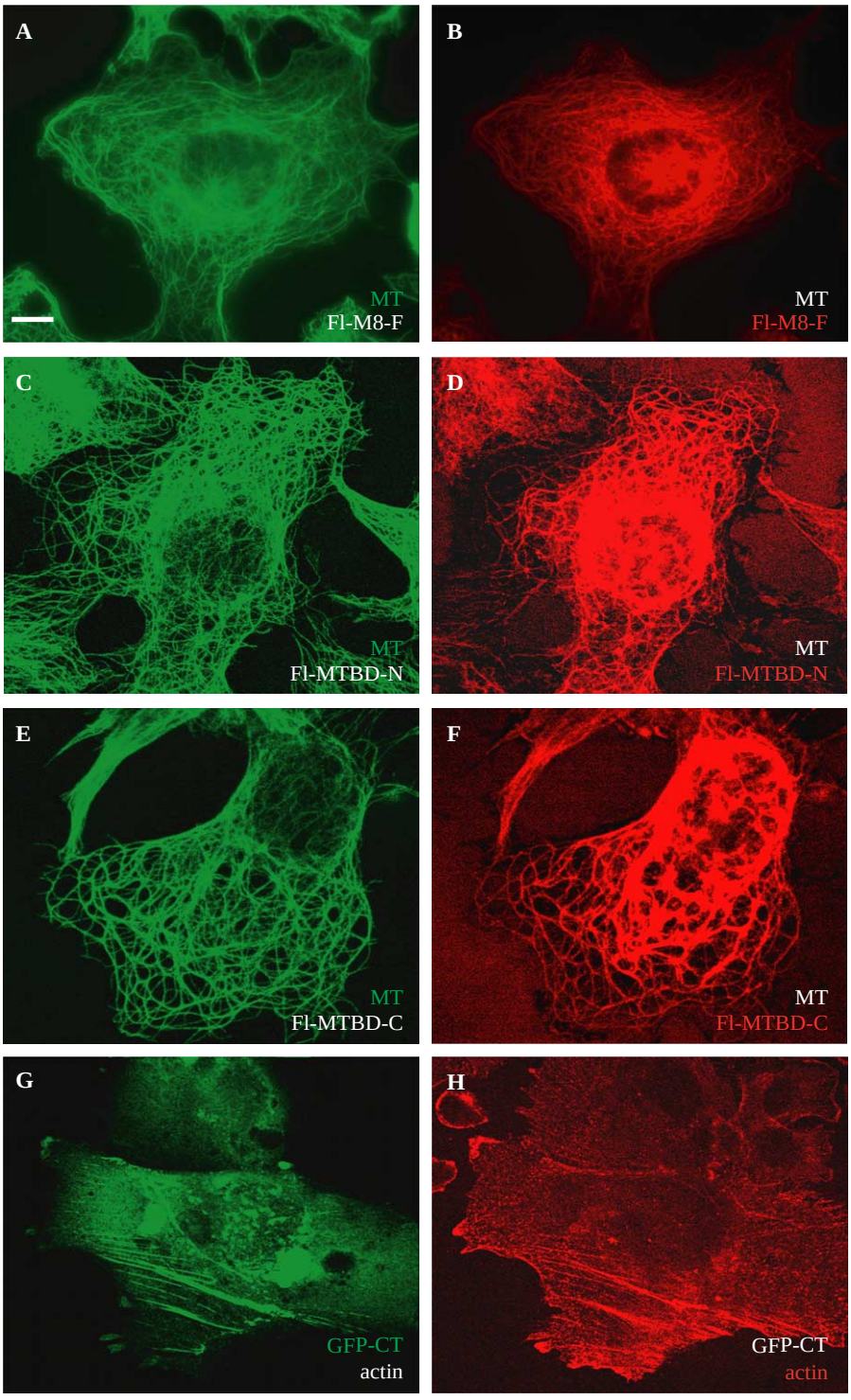

Fig. 3. MAP8 contains two microtubule binding domains. (A–F) COS7 cells were transfected with Flag-M8-F (A,B) or Flag-MTBD-N (C,D), or Flag-MTBD-C (E-F). 24–48 h post-transfection, the cells were subjected to double immunofluorescence microscopy using anti-tubulin (Sigma) (green in A, C, and E) and anti-Flag (red in B, D, and F). (G,H) The GFP-M8-CT transfected COS7 cells were double immunostained with anti GFP (G) and anti-actin (Sigma) (H). Bar represents 10 μm in all panels. (For interpretation of the references to color in this figure legend, the reader is referred to the web version of this paper.)

of MAP5/MAP1B light chain. This result is consistent with that reported for MAP1S [25]. Thus, MAP8 may possess the capability to associate with both microtubules and actin microfilaments.

To define further the direct binding activities of the two binding domains for microtubules, we conducted in vitro co-sedimentation assays using purified proteins. Both binding domains of HC (MTBD-N) and LC (MTBD-C) were

expressed in bacteria as GST fusion proteins, GST-MTBD-N and GST-MTBD-C (see diagram in Fig. 1B). The two purified recombinant fusion proteins were separately combined with purified microtubules (Cytoskeleton) for the binding assays. In the absence of microtubules, GST-MTBD-N (Fig. 4A) or GST-MTBD-C (not shown) remained in the soluble fraction after centrifugation at 100,000*g* (Fig. 4A, lane 5). In contrast, the majority of the fusion protein shifted from the supernatant to the pellet after addition of microtubules (Fig. 4A, lane 8). This binding between the MTBD domain and microtubules was specific: in parallel experiments with BSA (Fig. 4A, lanes 1–4) or GST (not shown), the control proteins remained in the supernatant in the presence or absence of microtubules (Fig. 4A, lanes 1 and 3). These analyses were repeated by three independent experiments.

To estimate the binding constant of this association, the co-sedimentation assays were repeated using a concentration range of GST-MTBD-N or GST-MTBD-C fusion protein. As expected, the association of GST-MTBD-N or GST-MTBD-C fusion protein with microtubules became saturated as the concentration of GST-MTBD-N (Fig. 4B) or GST-MTBD-C (not shown) fusion protein increased. A Scatchard plot of the data corresponding to three independent experiment sets yielded a k_d of 0.47 μM (Fig. 4C) for GST-MTBD-N binding to microtubules and a k_d of 1.38 μM for GST-MTBD-C (Fig. 4D). The k_ds of the two microtubule binding domains of MAP8 are within the range to those of other classical microtubule associated proteins [27,28]. Moreover, the microtubule binding domain in the HC appears to possess higher affinity than that in the LC. Our data define MAP8 contains two microtubule binding sites.

The N-terminus of heavy chain associates with the C-terminus of light chain to form MAP8 protein complex

We have demonstrated that MAP8 is cleaved in vivo into heavy and light chains, each containing a functional microtubule-binding domain. To understand whether MAP8 forms protein complex or the HC and LC function as two independent proteins, immunoprecipitation experiments were carried out using antibodies to either heavy or light chain to determine their relations in vivo. The resulting complexes co-immunoprecipitated by anti-M8-N or anti-M8-C were analyzed by immunoblots with anti-M8-C or anti-M8-N, respectively. While a sham antibody could not pull down either chain of MAP8 (Fig. 5A, lanes 2 and 4), the presence of both heavy and light chains detected in the immunoprecipitates using each antibody reveals that MAP8 forms a protein complex in vivo (Fig. 5A, lanes 1 and 3). To further define the sites responsible for the HC-LC association, we divided the HC into N- and C-terminal segments, M8-HC-N and M8-HC-C (see diagram in Fig. 1B). As stated previously, the HA epitope tagged N-terminal protein was distributed diffusely in the cytoplasm of the single transfected COS 7 cells (Fig. 5C).

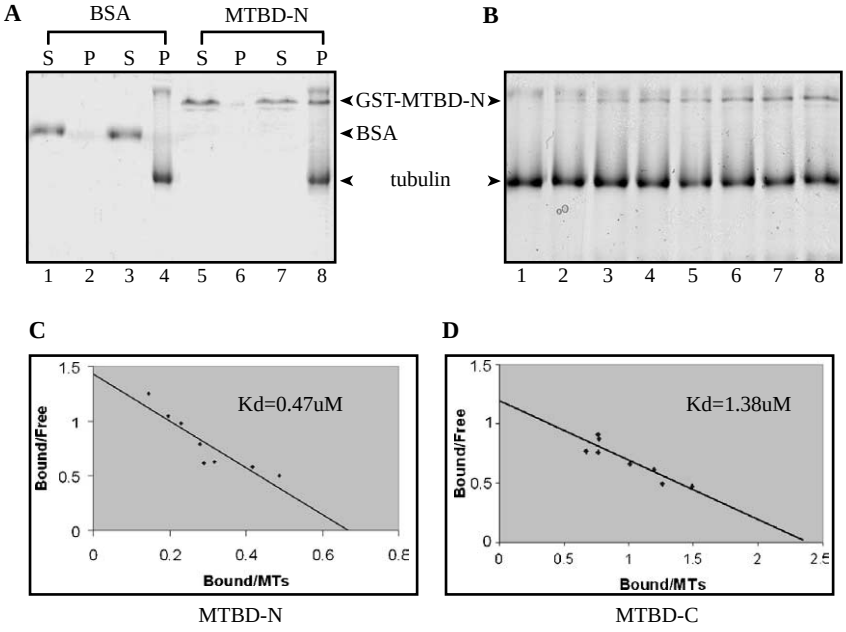

Fig. 4. Binding affinity assays of the two microtubule binding domains of MAP8. (A) Purified GST-MTBD-N protein co-sedimented with polymerized microtubules (lane 8), while it remained in supernatant in the absence of microtubules (lane 5). BSA control protein remains in soluble fraction with or without microtubules (lane 1 and 3). S, supernatant; P, pellet. (B) The GST-MTBD-N protein co-sedimented with microtubules was saturated while the concentration increased from 0.65 to 10.25 μM. (C,D) k_d of microtubule binding, Scatchard plot shows a k_d of 0.47 μM as binding affinity of the microtubule binding domain in the HC (MTBD-N) (C) and k_d of 1.38 μM for microtubule binding domain in the LC (MTBD-C) (D).

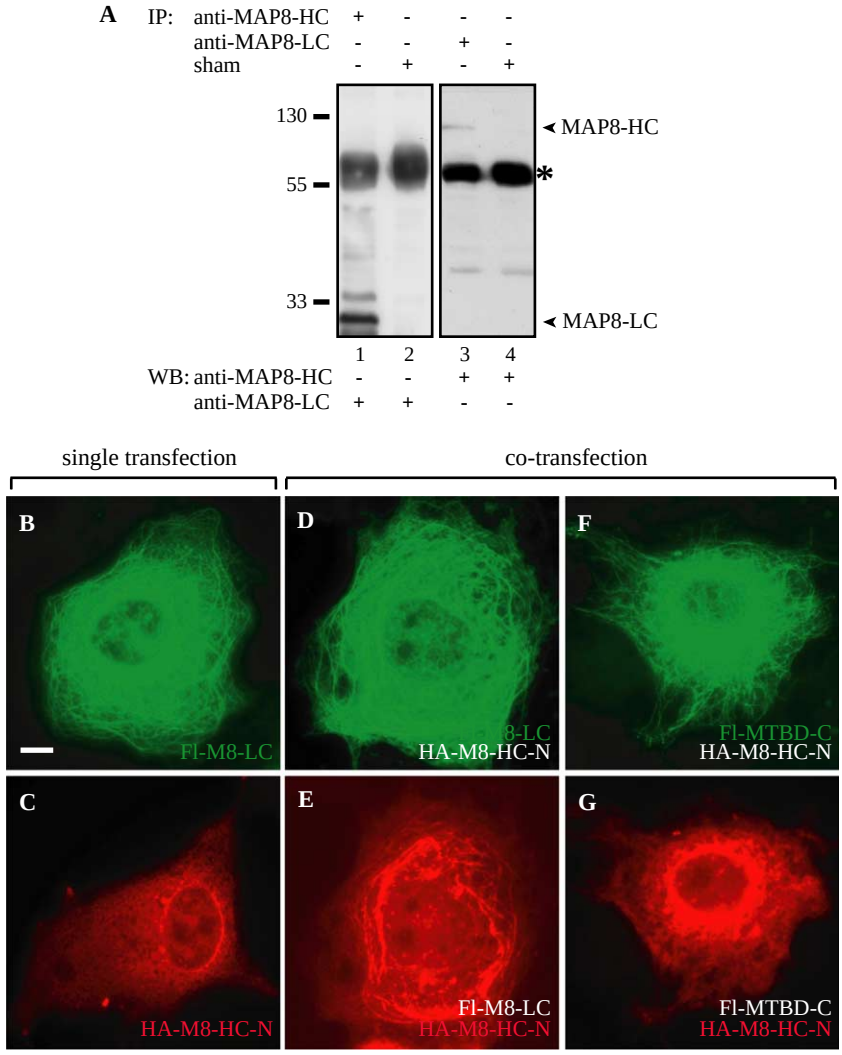

Fig. 5. N-terminus of the HC associates with C-terminus of the LC to form complex. (A) Immunoprecipitation assays on mouse brain lysates of 2 weeks. The total lysates were immunoprecipitated by anti-M8-N or a sham antibody followed by immunoblotting analysis with anti-M8-C (lanes 1 and 2). Likewise, anti-M8-C or a sham antibody was used for immunoprecipitations and anti-M8-N for immuno-detection (lanes 3 and 4). (B) Flag-MAP8-LC displays cytoskeletal network in transfected COS7 cells. (C) N-terminus of the HA-MAP8-HC distributes diffusely in the cytoplasm of the single transfected cells. (D,E) N-terminus of HA-MAP8-HC co-localizes with flag-MAP8-LC on microtubules when co-expressed with the LC in the cells. (F,G) When C-terminus of the LC was deleted, N-terminus of the HA-MAP8-HC lost its association with the LC on microtubules. Bar represents 8 μm in all panels.

In contrast, the flag tagged MAP8-LC containing microtubule binding domain decorates cytoskeletal network (Fig. 5B). Notably, when co-transfected with flag-MAP8-LC, the N-terminus of HC co-localizes with the LC protein, displaying a filamentous array (Figs. 5D and E). However, the association of the N-terminus of HC with the LC on microtubule network was lost when the C-terminal sequence of the LC was deleted (Figs. 5F and G). These data demonstrate that N-terminus of the HC and C-terminus of the LC contain the binding sites for forming the protein complex.

Discussion

Our results define MAP8 as a true microtubule associated protein containing two microtubule binding domains. This conclusion is supported by several lines of evidence including co-localization of MAP8 with microtubules in transfected cells and the direct binding capability with purified microtubules in vitro. A recent study on MAP1S (MAP8) also showed the C-terminal light chain could co-localize with microtubules in transfected cells [25]. This report identifies the second microtubule binding site and characterizes the binding affinities for both microtubule binding domains, which defines MAP8 as a novel classical microtubule associated protein. Our study improves our understanding of constituents of the cytoskeletal complex.

Recent studies on microtubule-associated proteins provide a new view that various microtubule-related proteins might be inter-regulated and non-motor microtubule binding proteins can affect the access of microtubules for certain microtubule-based motor proteins. Upregulation or

perturbation of MAPs may be a causative factor for neurodegeneration and cell death in many human disorders, including Parkinson's, Alzheimer's, ALS, and mental retardation in fragile X syndrome [19,23,24,29,30]. However, the mechanisms underlying cell death mediated by MAPs overexpression require further elucidation. The association of MAP8 with both actins and microtubules implies that MAP8 could be also involved in actin-related functions. Similar related functions of classical MAPs have been proposed to serve a critical role in neuromorphogenesis. However, little information is currently available about the precise organization or coordination of microtubules and actins during different functional events in neurons. In fact, it was proposed that MAPs interacting with both the microtubule and actin cytoskeletons are good candidates to play a major role in certain cellular processes, such as cell motility and neurite initiation (review see [31]). It is also tempting to speculate that MAP8 could be one of the key players in various cellular events by altering microtubule function, for example by stabilizing polymers and forming bundles, or by targeting signaling molecules from the actin to the microtubule domain. The identification and characterization of MAP8 provide a new candidate for future studies of pathogenesis.

Acknowledgments

We gratefully acknowledge Dr. Chengbiao Wu and Mr. Steve Kaiser for scientific discussions and technical assistance. This work was supported by Muscular Dystrophy Association Research Grant and NIH Grants NS42791 and NS43281 for Y. Yang.

References

[1] K. Andra, B. Nikolic, M. Stocher, D. Drenckhahn, G. Wiche, Genes Dev. 12 (1998) 3442–3451.
[2] R.A. Nixon, I. Fischer, S.E. Lewis, J. Cell Biol. 110 (1990) 437–448.
[3] C.C. Garner, A. Garner, G. Huber, C. Kozak, A. Matus, J. Neurochem. 55 (1990) 146–154.
[4] B. Pedrotti, K. Islam, FEBS Lett. 388 (1996) 131–133.
[5] B. Pedrotti, L. Ulloa, J. Avila, K. Islam, Biochemistry 35 (1996) 3016–3023.
[6] M. Togel, G. Wiche, F. Propst, J. Cell Biol. 143 (1998) 695–707.
[7] J. Ding, J.J. Liu, A.S. Kowal, T. Nardine, P. Bhattacharya, A. Lee, Y. Yang, J. Cell Biol. 158 (2002) 427–433.
[8] R. Franzen, S.L. Tanner, S.M. Dashiell, C.A. Rottkamp, J.A. Hammer, R.H. Quarles, J. Cell Biol. 155 (2001) 893–898.
[9] C. Sanchez, M. Perez, J. Avila, Eur. J. Cell Biol. 79 (2000) 252–260.
[10] D.W. Cleveland, S.Y. Hwo, M.W. Kirschner, J. Mol. Biol. 116 (1977) 227–247.
[11] Y. Takei, S. Kondo, A. Harada, S. Inomata, T. Noda, N. Hirokawa, J. Cell Biol. 137 (1997) 1615–1626.
[12] W. Edelmann, M. Zervas, P. Costello, L. Roback, I. Fischer, J.A. Hammarback, N. Cowan, P. Davies, B. Wainer, R. Kucherlapati, Proc. Natl. Acad. Sci. USA 93 (1996) 1270–1275.
[13] C. Gonzalez-Billault, E.M. Jimenez-Mateos, A. Caceres, J. Diaz-Nido, F. Wandosell, J. Avila, J. Neurobiol. 58 (2004) 48–59.
[14] A. Meixner, S. Haverkamp, H. Wassle, S. Fuhrer, J. Thalhammer, N. Kropf, R.E. Bittner, H. Lassmann, G. Wiche, F. Propst, J. Cell Biol. 151 (2000) 1169–1178.
[15] J. Teng, Y. Takei, A. Harada, T. Nakata, J. Chen, N. Hirokawa, J. Cell Biol. 155 (2001) 65–76.
[16] T. Takano, C. Sawai, Y. Takeuchi, J. Child Neurol. 19 (2004) 107–115.
[17] A. Harada, K. Oguchi, S. Okabe, J. Kuno, S. Terada, T. Ohshima, R. Sato-Yoshitake, Y. Takei, T. Noda, N. Hirokawa, Nature 369 (1994) 488–491.
[18] A. Ebneth, R. Godemann, K. Stamer, S. Illenberger, B. Trinczek, E. Mandelkow, J. Cell Biol. 143 (1998) 777–794.
[19] J. Lewis, E. McGowan, J. Rockwood, H. Melrose, P. Nacharaju, M. Van Slegtenhorst, K. Gwinn-Hardy, M. Paul Murphy, M. Baker, X. Yu, K. Duff, J. Hardy, A. Corral, W.L. Lin, S.H. Yen, D.W. Dickson, P. Davies, M. Hutton, Nat. Genet. 25 (2000) 402–405.
[20] D. Panda, J.C. Samuel, M. Massie, S.C. Feinstein, L. Wilson, Proc. Natl. Acad. Sci. USA 100 (2003) 9548–9553.
[21] J.Q. Trojanowski, V.M. Lee, Med. Clin. North America 86 (2002) 615–627.
[22] N.J. Cairns, V.M. Lee, J.Q. Trojanowski, J. Pathol. 204 (2004) 438–449.
[23] V. Brown, P. Jin, S. Ceman, J.C. Darnell, W.T. O'Donnell, S.A. Tenenbaum, X. Jin, Y. Feng, K.D. Wilkinson, J.D. Keene, R.B. Darnell, S.T. Warren, Cell 107 (2001) 477–487.
[24] R. Lu, H. Wang, Z. Liang, L. Ku, W.T. O'Donnell, W. Li, S.T. Warren, Y. Feng, Proc. Natl. Acad. Sci. USA 101 (2004) 15201–15206.
[25] Z. Orban-Nemeth, H. Simader, S. Badurek, A. Trancikova, F. Propst, J. Biol. Chem. 280 (2005) 2257–2265.
[26] M. Togel, R. Eichinger, G. Wiche, F. Propst, FEBS Lett. 451 (1999) 15–18.
[27] R.L. Coffey, D.L. Purich, J. Biol. Chem. 270 (1995) 1035–1040.
[28] K.T. Wallis, S. Azhar, M.B. Rho, S.A. Lewis, N.J. Cowan, D.B. Murphy, J. Biol. Chem. 268 (1993) 15158–15167.
[29] D.W. Dickson, Am. J. Pathol. 151 (1997) 7–11.
[30] D.W. Dickson, J. Neuropathol. Exper. Neurol. 56 (1997) 321–339.
[31] L. Dehmelt, S. Halpain, J. Neurobiol. 58 (2004) 18–33.